

SN DUST YIELDS-FALLBACK, METALLICITY AND ROTATION IMPACT

S. Marassi^{1,★}, R. Schneider¹, M. Limongi^{1,2}, A. Chieffi³, M. Bocchio^{1,4,5}, S. Bianchi⁴

¹INAF/Osservatorio Astronomico di Roma, Via di Frascati 33, 00040 Monte Porzio Catone, Italy

²Kavli Institute for the Physics and Mathematics of the Universe, Todai Institutes for Advanced Study, The University of Tokyo, Kashiwa 277-8583, Japan

³INAF/IASF, Via Fosso del Cavaliere 100, 00133 Roma, Italy

⁴INAF/Osservatorio Astrofisico di Arcetri, Largo Enrico Fermi 5, 50125 Firenze, Italy

⁵Institut d'Astrophysique Spatiale (IAS), Université Paris-Sud France

★E-mail: stefania.marassi@oa-roma.inaf.it

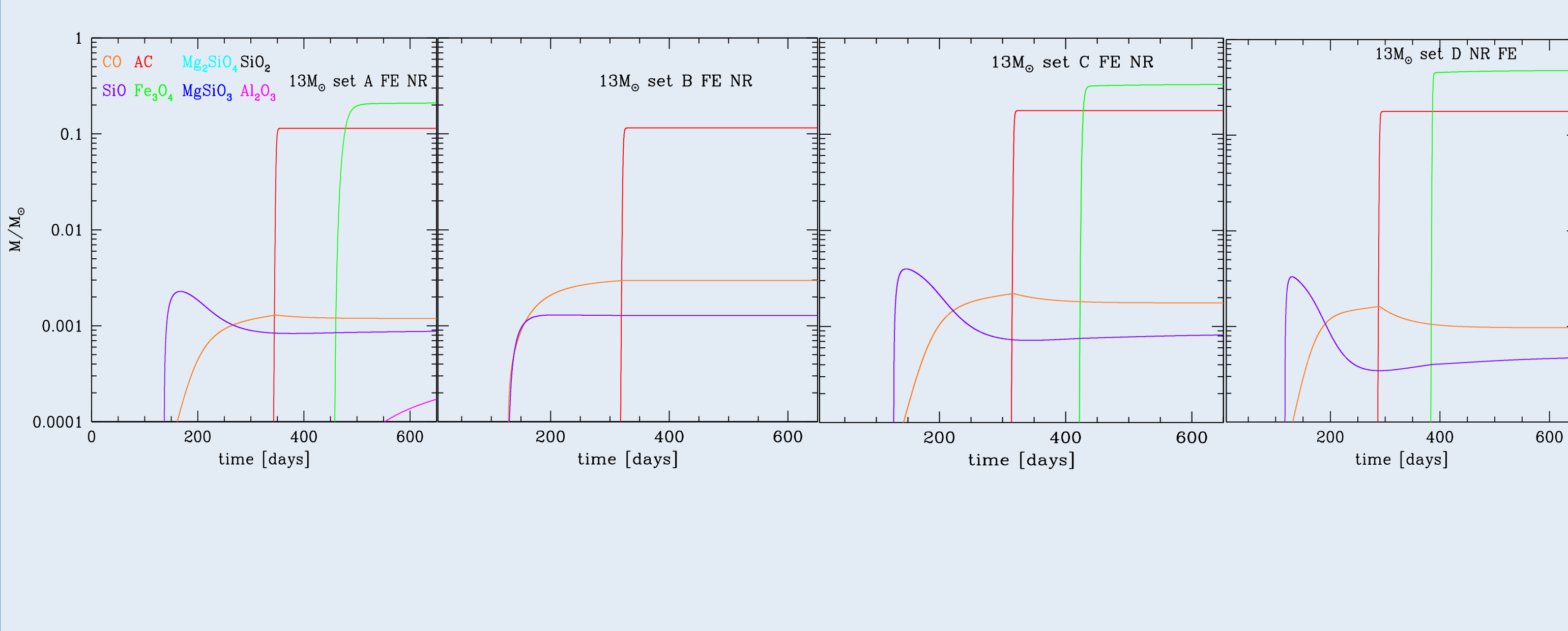


ABSTRACT

In astrophysical environments dust is an important ingredient and it regulates the physical and chemical conditions in interstellar medium. Sites of dust formation are the expanding ejecta of core-collapse SNe. The goal of this study is to provide, for the first time, a dust mass grid, which takes into account the great diversity of SN event, spanning a large range of progenitor masses and including the detailed study of impact of three key ingredients on the ejecta: rotation, metallicity and fallback. The calculation of dust formation in the ejecta is based on classical nucleation theory. The onset of grain condensation is controlled by the temperature and the density in the ejecta, whereas the grain composition depends on the nature of the SN progenitor. As the ejecta expands we follow the formation/destruction processes involving molecules, which play an important role in subtracting gas-phase elements, and the condensation of seven different grain species, amorphous carbon (AC), iron (Fe), corundum(Al_2O_3), magnetite(Fe_3O_4), enstatite(MgSiO_3), fosterite(Mg_2SiO_4), and quartz(SiO_2). We also investigate metal and dust yields released by the first SNe with the aim to reproduce the properties of the environment out of which the most metal-poor stars have formed. Dust formation calculations are performed assuming both unmixed and uniformly mixed initial composition within the He core and varying the mass cut and explosion energies so as to reproduce the observed elemental composition of carbon-normal and carbon-enhanced metal poor stars.

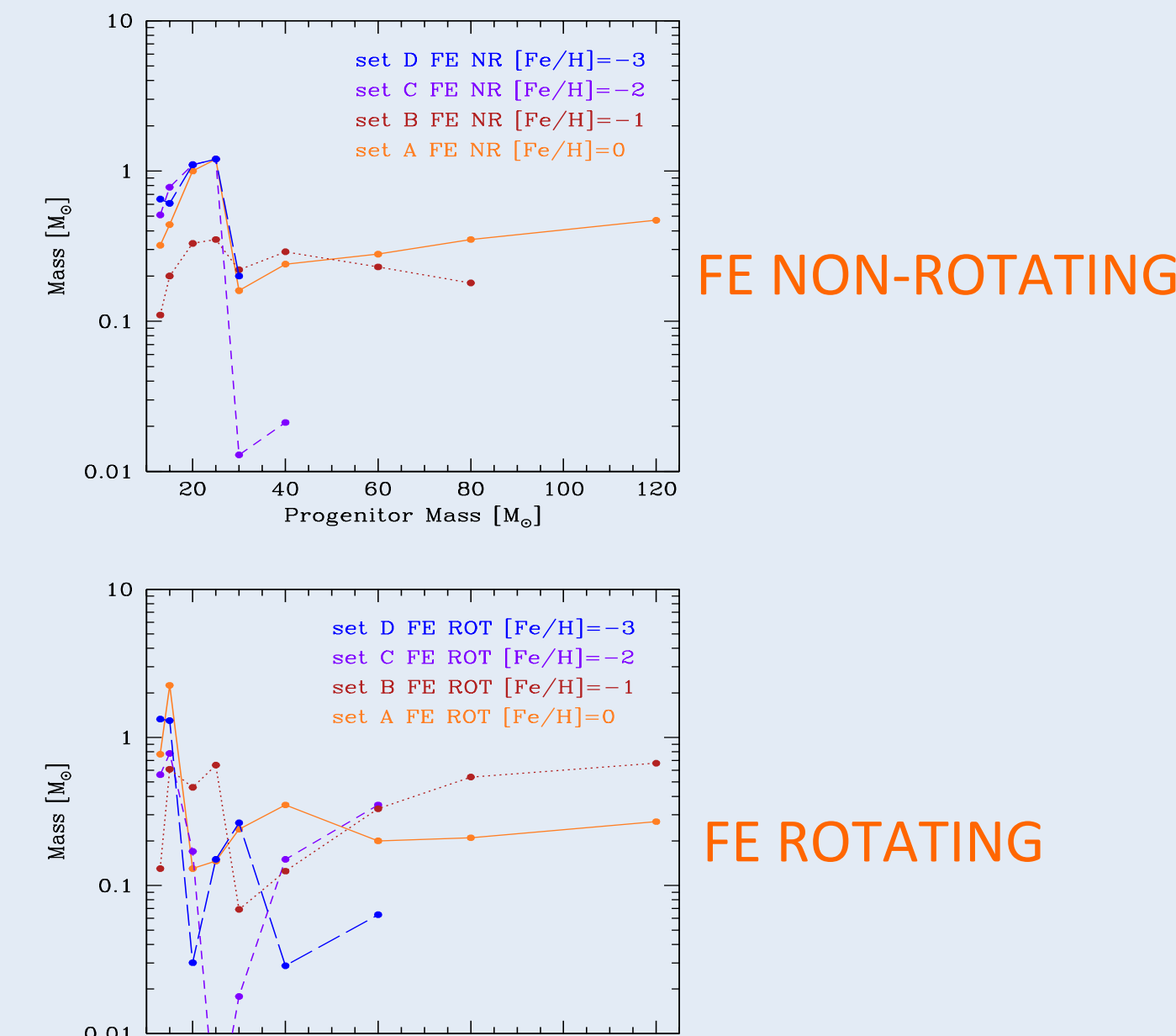
TIME EVOLUTION OF DUST MASS AND MOLECULES

FIXED ENERGY MODELS (FE): time evolution of molecular and dust masses for a $13M_{\odot}$ progenitor at different metallicity: $[\text{Fe}/\text{H}] = 0$ (set A), -1 (set B), -2 (set C), -3 (set D)

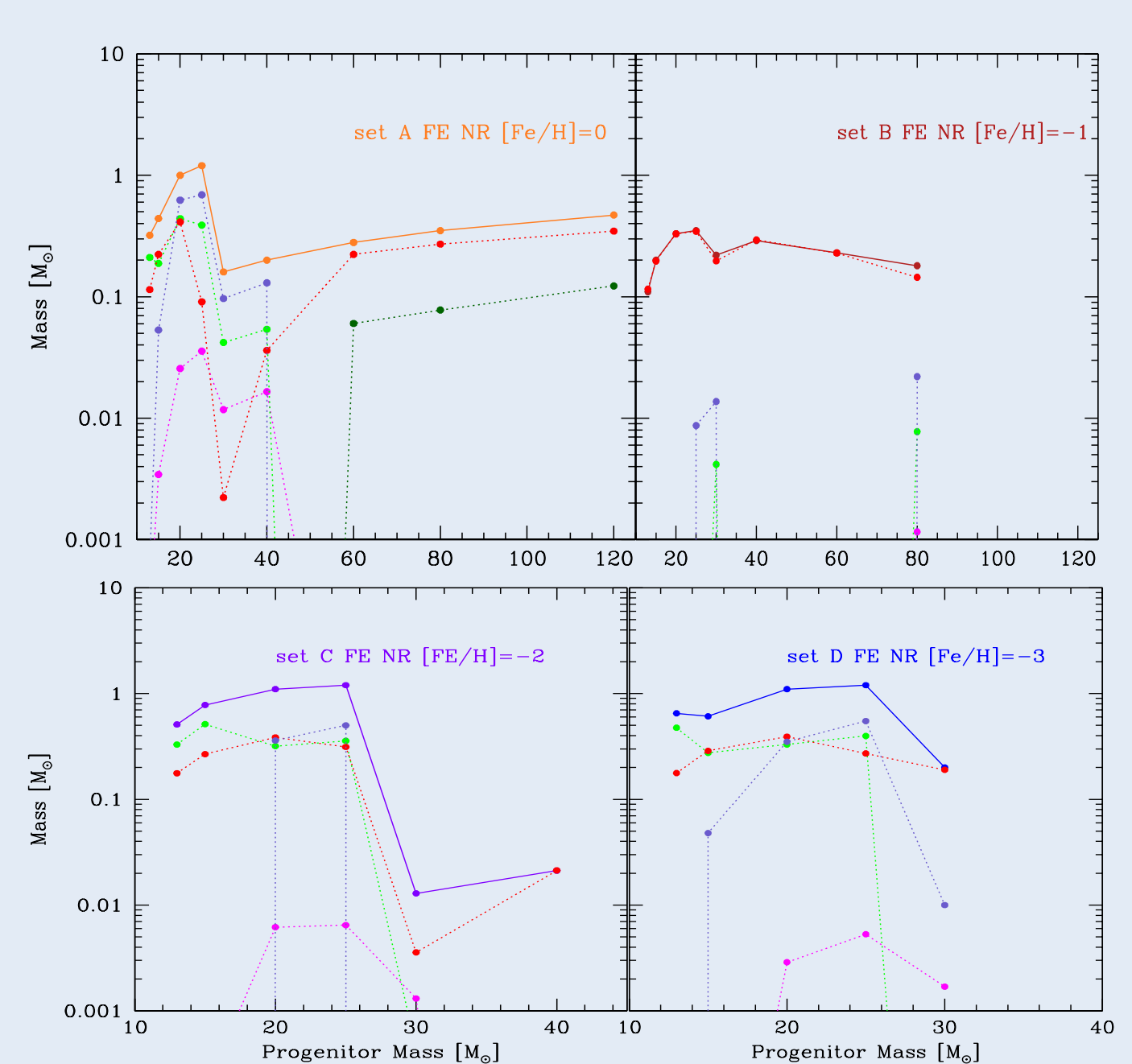


SN DUST YIELDS FROM SOLAR TO SUB-SOLAR METALLICITY

FIXED ENERGY MODELS(FE): Mass of dust condensed in the ejecta of non-rotating and rotating SN models for 4 value of metallicity.

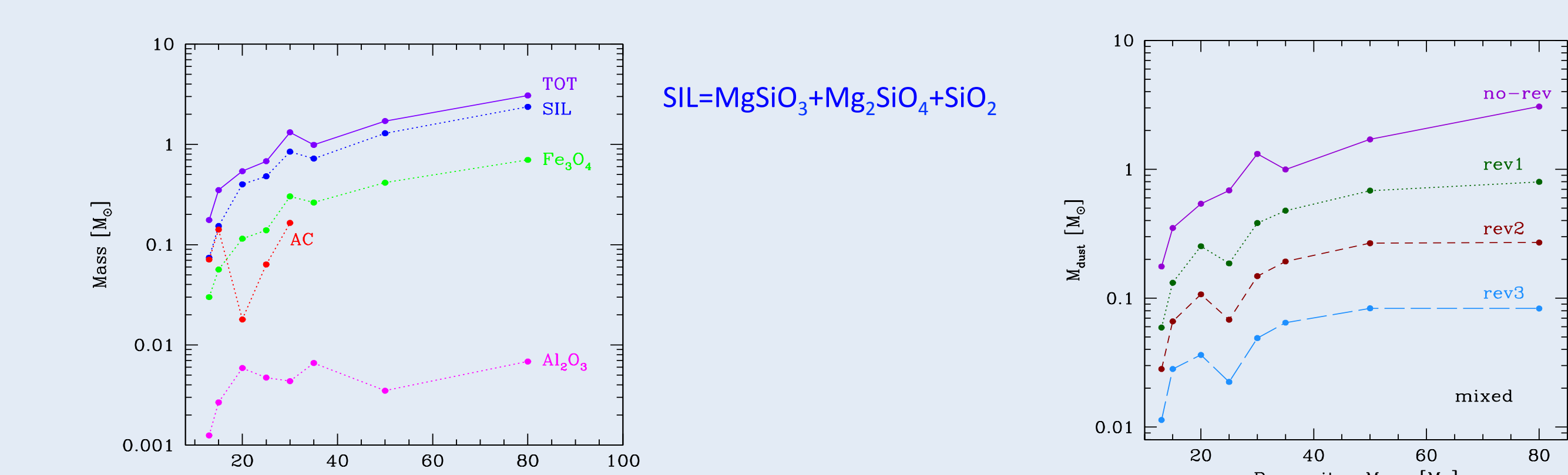


FIXED ENERGY MODELS(FE): Mass of dust grains condensed in non-rotating SN models for 4 value of metallicity.



TOTAL DUST BUDGET FOR POP III SN

We use detailed pre-supernova and supernova explosion models for metal free stellar progenitors with mass ranging between 13 to 80 solar masses developed by Limongi & Chieffi (2012). We choose the mass cut that provides the best fit of the yields of the Cayrel average star (Cayrel et al. 2004). For all Pop III ejecta models the thermal evolution follow an adiabatic expansion normalized to the output of SN explosion simulations.

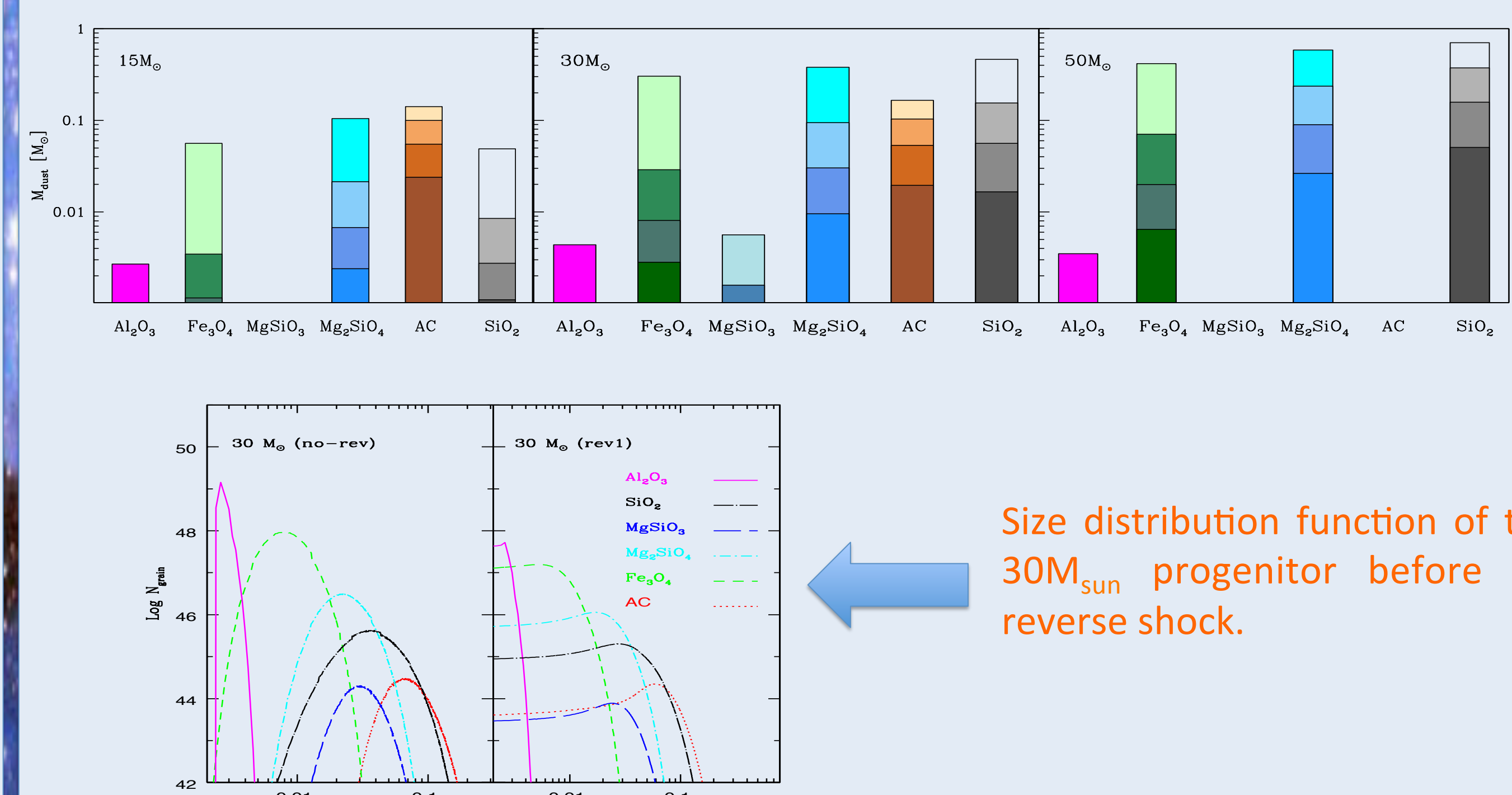


Mass of dust grains before the passage of the reverse shock as a function of the progenitor mass.

The mass of dust grains at the end of nucleation and after the passage of the reverse shock of increasing intensity, as a function of the progenitor mass.

REVERSE SHOCK IMPACT ON DUST MASS AND GRAIN SIZE DISTRIBUTION

Histograms showing the mass of dust in the different compounds at the end of nucleation and after the passage of the reverse shock of increasing intensity for three progenitors.

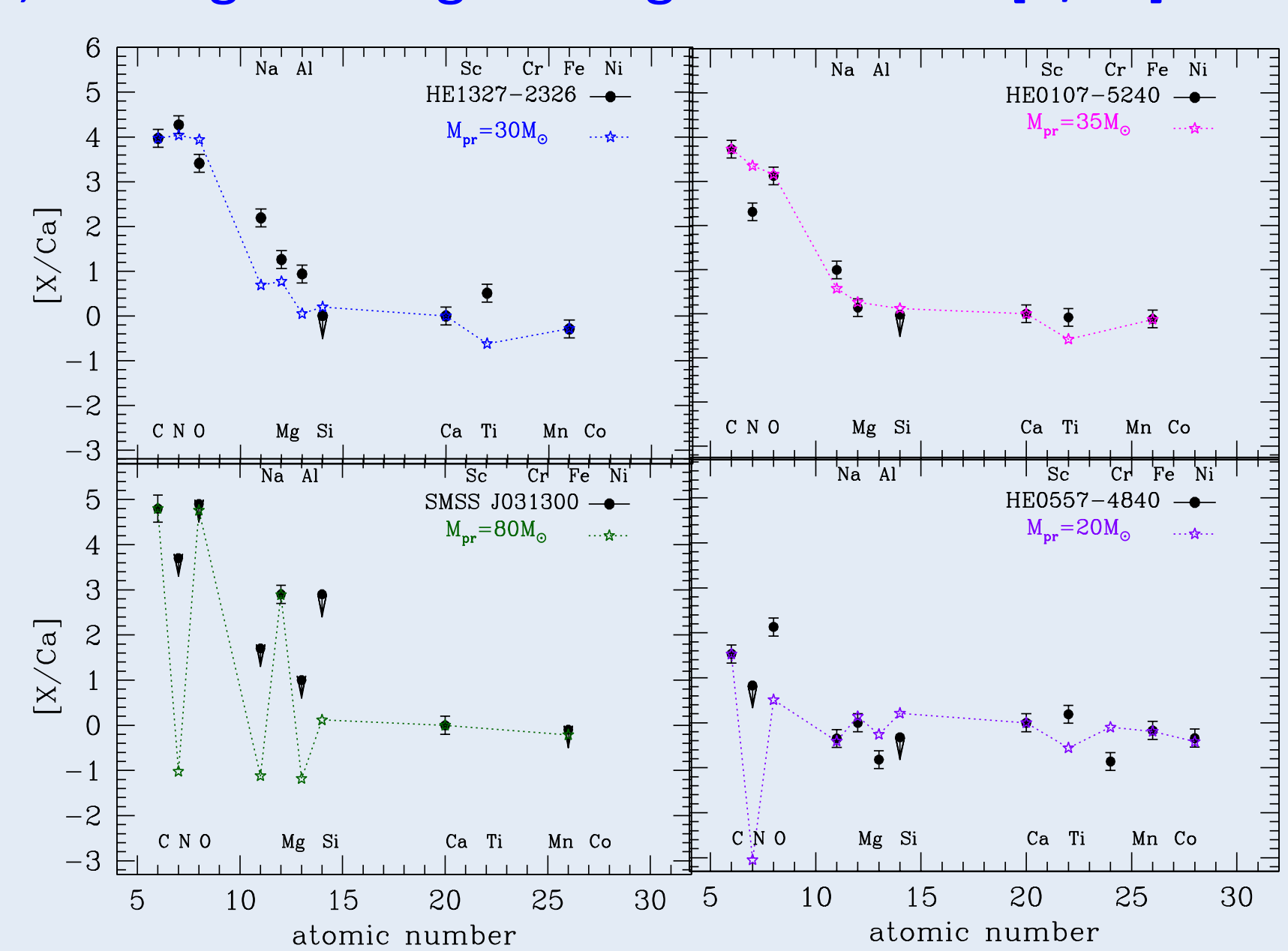


Size distribution function of the grains for a $30M_{\odot}$ progenitor before and after the reverse shock.

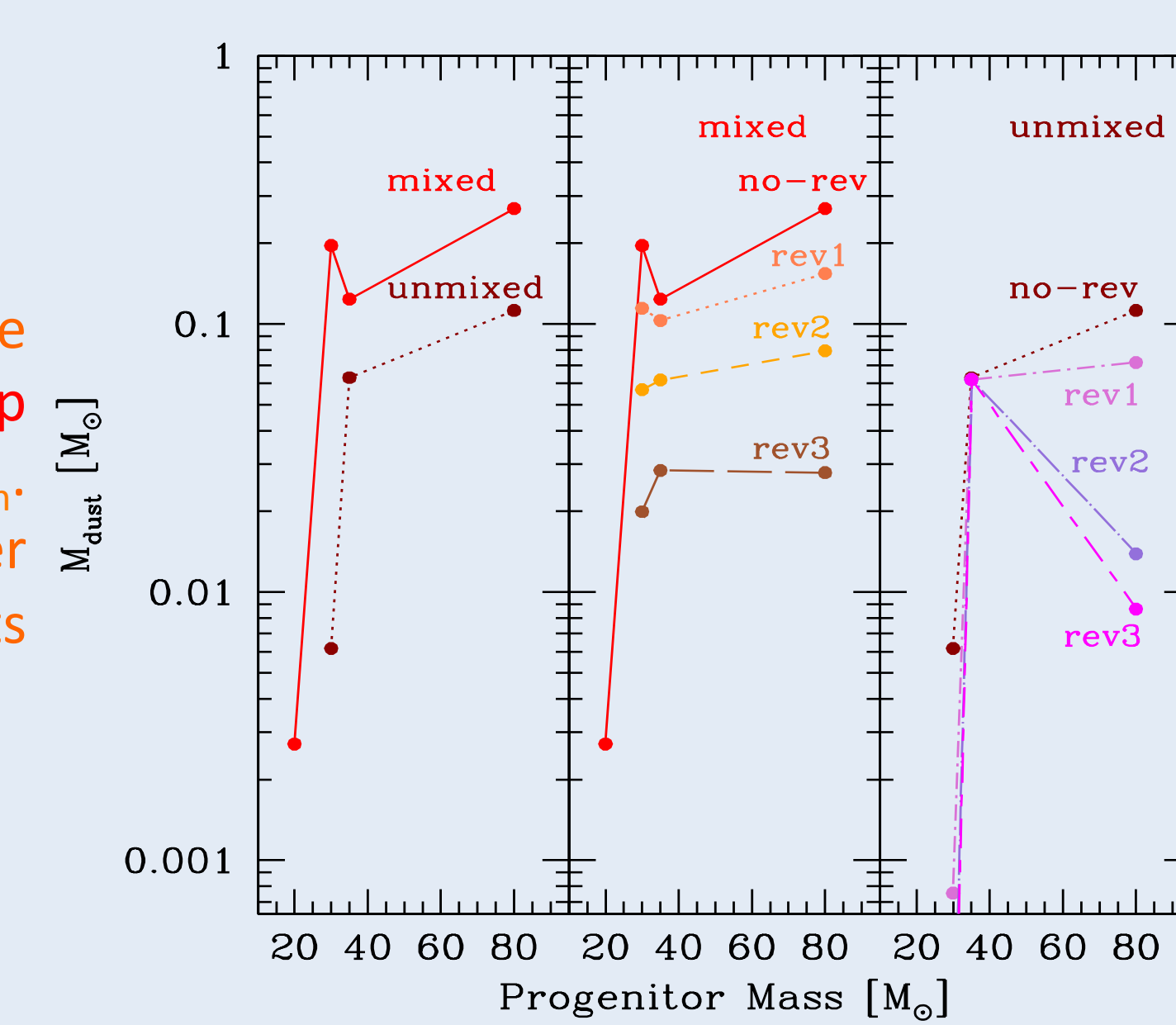
For the reverse shock calculation see Marco Bocchio's poster

TOTAL DUST BUDGET FOR C-ENHANCED HYPER-IRON-POOR STARS

We investigate a possible formation scenario for hyper-iron poor stars. As suggested by Umeda & Nomoto (2002) we use mixing and fallback model: during the SN explosion internal mixing occurs up to a small region outside the mass cut; a small amount of the mixed material is expelled from the star with most of it falling back into the central region, leading to a large enough fraction of [C/Fe].



Comparison between the observed elemental abundance ratios of hyper-iron poor stars and the chemical yields of Pop III faint SN with progenitor masses of 30, 35, 20 and 80 M_{\odot} . Mixing and fallback are chosen so as to minimize the scatter with the observations. Dots with arrows show upper limits and filled points with errorbars indicate the detections.



The only grain species that forms in faint Pop III SN ejecta is amorphous carbon. In the figure we plots the mass of AC at the end of nucleation for mixed and unmixed ejecta models and after the passage of reverse shock of increasing intensity.

MAIN RESULTS AND CONCLUSIONS

- From FE models we learn that the fallback affects the composition and mass of the dust grains depending on the metallicity
- Rotation enhances the dust mass in lower mass SN progenitors but also increase the remnant mass leading to a formation of AC grains.
- Ordinary core-collapse Pop III SNe are efficient dust producers: the dust mass ranges between $[0.18-3]M_{\odot}$ and it is dominated by silicates.
- We estimate metal yields and dust produced in faint Pop III SN explosions fitting the elemental abundances on the surface of C-enhanced hyper-iron-poor-stars
- Faint Pop III SNe produce dust, but contrary to ordinary core collapse SNe, the only grain species that forms in the ejecta is Amorphous Carbon
- The amount of dust formed depends on the reverse shock strength and on the mixing efficiency

REFERENCES

- Marassi et al., 2014, ApJ, 794, 100
 Marassi et al., 2015, MNRAS, 454, 4250
 Bocchio et al., 2016, A&A, 587, 157 [see Poster]
 Umeda & Nomoto, 2002, ApJ, 565, 385
 Chiaki et al., 2014, MNRAS, 439, 3121
 Limongi & Chieffi, 2012, ApJS, 199, 38L
 Limongi & Chieffi, 2016, in preparation
 Marassi et al., 2016, in preparation